



Influence of chitosan coating on magnetic nanoparticles in endothelial cells and acute tissue biodistribution

Mariela Agotegaray, Adrián Campelo, Roberto Zysler, Fernanda Gumilar, Cristina Bras, Alejandra Minetti, Virginia Massheimer & Verónica Lassalle

To cite this article: Mariela Agotegaray, Adrián Campelo, Roberto Zysler, Fernanda Gumilar, Cristina Bras, Alejandra Minetti, Virginia Massheimer & Verónica Lassalle (2016): Influence of chitosan coating on magnetic nanoparticles in endothelial cells and acute tissue biodistribution, Journal of Biomaterials Science, Polymer Edition, DOI: [10.1080/09205063.2016.1170417](https://doi.org/10.1080/09205063.2016.1170417)

To link to this article: <http://dx.doi.org/10.1080/09205063.2016.1170417>



Published online: 02 Jun 2016.



Submit your article to this journal [↗](#)



Article views: 1



View related articles [↗](#)



View Crossmark data [↗](#)

Influence of chitosan coating on magnetic nanoparticles in endothelial cells and acute tissue biodistribution

Mariela Agotegaray^a, Adrián Campelo^b, Roberto Zysler^c, Fernanda Gumilar^b, Cristina Bras^b, Alejandra Minetti^b, Virginia Massheimer^b and Verónica Lassalle^a

^aINQUISUR, UNS, CONICET, Departamento de Química, Universidad Nacional del Sur, Avda. Alem 1253, B8000CPB, Bahía Blanca, Argentina; ^bINBIOSUR, UNS, CONICET, DBByF, Universidad Nacional del Sur, San Juan 670, 8000, Bahía Blanca, Argentina; ^cCNEA, Centro Atómico Bariloche, Div. Resonancias Magnéticas, CONICET, Avda. Bustillo Km. 9,5, 8400 - San Carlos de Bariloche, Argentina

ABSTRACT

Chitosan coating on magnetic nanoparticles (MNPs) was studied on biological systems as a first step toward the application in the biomedical field as drug-targeted nanosystems. Composition of MNPs consists of magnetite functionalized with oleic acid and coated with the biopolymer chitosan or glutaraldehyde-cross-linked chitosan. The influence of the biopolymeric coating has been evaluated by *in vitro* and *in vivo* assays on the effects of these MNPs on rat aortic endothelial cells (ECs) viability and on the random tissue distribution in mice. Results were correlated with the physicochemical properties of the nanoparticles. Nitric oxide (NO) production by ECs was determined, considering that endothelial NO represents one of the major markers of ECs function. Cell viability was studied by MTT assay. Different doses of the MNPs (1, 10 and 100 µg/mL) were assayed, revealing that MNPs coated with non-cross-linked chitosan for 6 and 24 h did not affect neither NO production nor cell viability. However, a significant decrease in cell viability was observed after 36 h treatment with the highest dose of this nanocarrier. It was also revealed that the presence and dose of glutaraldehyde in the MNPs structure impact on the cytotoxicity. The study of the acute tissue distribution was performed acutely in mice after 24 h of an intraperitoneal injection of the MNPs and sub acutely, after 28 days of weekly administration. Both formulations greatly avoided the initial clearance by the reticuloendothelial system (RES) in liver. Biological properties found for N1 and N2 in the performed assays reveal that chitosan coating improves biocompatibility of MNPs turning these magnetic nanosystems as promising devices for targeted drug delivery.

ARTICLE HISTORY

Received 29 January 2016
Accepted 22 March 2016

KEYWORDS

Magnetic carriers;
nanoparticles; chitosan;
endothelial cells;
biodistribution

1. Introduction

Major problem scientists are facing in the treatment of localized diseases such as cancer or rheumatoid arthritis is that the drugs injected in the body spread through the circulatory

system, not only to the diseased area, but also to healthy tissues. Therefore, the need for a targeted treatment based on controlled delivery of the drug to the desired organ led to the development of such enhanced and more efficient methods and devices. In particular, magnetic nanoparticles (MNPs) have been developed along last decades aiming to contribute to solve this kind of limitations in the biomedical field. The superparamagnetic property of these nanosystems enables their external manipulation under the influence of a magnetic field.[1,2]

A precise knowledge about the effect of MNPs on normal cells and tissue distribution in the body is critical as a pre-clinical setting before any potential use. In fact, this is one of the main reasons limiting the commercialization of MNPs in a massive way.[3]

Once MNPs enter the body, they should be able to overpass endothelial cells (ECs) barrier in order to reach the desired organ or tissue for treatment. The vascular endothelium is a cell monolayer located between the vessel wall and the blood. It acts as a selective barrier between blood and surrounding tissues which enables cellular exchange of nutrients, biochemical factors and waste products. The endothelium exhibits a pivotal role in the maintenance of vascular homeostasis through its antithrombotic and antiatherogenic properties. These functions depend on the ability to produce vasoactive compounds such as nitric oxide (NO) and prostacyclin.[4] The studies regarding the influence of MNPs coating on ECs are very limited when comparing with the huge amount of information on MNPs actually published in the available literature. Only Ge et al. [5] analyzed the cytotoxic effects of dimercaptosuccinic acid-coated hematite ($\alpha\text{-Fe}_2\text{O}_3$) nanoparticles employing human aortic endothelial cells (HAECs) as experimental model. They described a dose-dependent cytotoxicity in concentrations ranging from 0.001 to 0.2 mg/mL. They reported that concentrations up to 0.02 mg/mL of these MNPs had little toxic effect on HAECs.

Even though there are many studies concerning MNPs biodistribution, further research is required to achieve a complete evaluation of the *in vivo* behavior. Reports studying MNPs with diverse coatings, propose several mechanisms for the tissue distribution of MNPs.[6–8] Factors such as the route of administration, physicochemical properties of the nanoparticles and the physiological environment where nanocarriers are introduced, appear as relevant to define the biodistribution. Among others, particle size, shape, and surface charge are the main properties of MNPs influencing biodistribution.[9] Such properties strongly depend on the coating selected to modify the magnetic core.[10,11]

The aim of this work is to investigate the influence of the biopolymeric chitosan coating of MNPs on ECs as well as on acute and sub acute biodistribution, after 24 h and after 28 days of weekly administration, respectively. These aspects are considered relevant as a first step toward their therapeutic biomedical application. To do this, two magnetic naocarriers were tested: both composed of magnetite, oleic acid, and chitosan; and one of them also include glutaraldehyde as biopolymer cross-linker. Such formulations were optimized regarding to the physicochemical properties of interest, i.e. polydispersity, surface charge, and ability to bind to a model drug (Diclofenac).[12,13] Then this contribution proposes the following step in view of the practical implementation of these nanosystems as targetable drug delivery systems related to pre-clinical studies at vascular and biodistribution levels.

As far as authors' knowledge, a study of this nature has not been reported earlier in the open literature combining the set of variables, materials and experiments here proposed. Only one research has studied the biodistribution of magnetic chitosan nanosystems. Kim et al. [14] prepared nanosized magnetite by spray-coprecipitation methodology, achieving

sizes of 9.5 nm for the magnetite core. Then, dispersions were prepared from this magnetite mixed with different chitosan proportions. The tissue biodistribution of intravenous-injected chitosan-magnetite mixture was studied by intraoral X-ray equipment and inductively coupled plasma-atomic emission spectrometer. Their results indicated that the systems were mainly distributed to liver and kidney. The research study here presented reinforces the effect of chitosan coating on magnetite-core nanosystems over acute biodistribution, revealing that not only the coating is a key factor in the distribution profile, but also the controlled nano-size, stability of coating as well as the employment of a specific methodology to the determination of MNPs on each organ.

2. Materials and methods

2.1. Materials

Trypsin/EDTA (10×), l-glutamine (100×), amphotericin B (0.25 mg/mL), and penicillin/streptomycin (100×) were obtained from PAA Laboratories (Pasching, Austria). Fetal calf serum (FCS) was purchased from Natocor Argentina. Griess reagents were purchased from Britannia Laboratories (Buenos Aires, Argentina). Dulbecco's modified Eagle's medium (DMEM), MPA, and all other reagents were purchased from Sigma Chemical Company (St Louis, MO, USA).

2.2. Synthesis, morphological, and magnetic characterization of the MNPs

Magnetite nanoparticles stabilized with oleic acid were synthesized by the co-precipitation method, according with the methodology previously studied.[12,13] Briefly, 0.3 g of oleic acid (OA) were added, under nitrogen atmosphere and at 70 °C, to 20 mL of an aqueous solution composed by $\text{FeSO}_4 \cdot 7\text{H}_2\text{O}$ and $\text{FeCl}_3 \cdot 6\text{H}_2\text{O}$ ($\text{Fe}^{2+}/\text{Fe}^{3+}$) with an iron molar ratio equal to 0.5. Then, 5 mL of NaOH 5 M were added dropwise. After 30 min of reaction, the precipitate was washed three times with water and dried at 45 °C. The nanoprecipitation method was employed to modify the MNPs with chitosan as previously described [7]: 300 mg of the MAG/OA MNPs were dispersed in 75 mL of acetone. After 15 min of sonication, 15 mL of an aqueous dissolution of chitosan (CS) (10.0 mg / mL) in acetic acid were added. The resulting solid was magnetically separated with a high-power Nd magnet, washed three times with water, and dried at 45 °C for 24 h. The MNPs obtained from this formulation are named N1 (MAG/OA/CS) hereafter. Cross-linking of polymeric chains with glutaraldehyde (GA) was performed to fix CS to the magnetic core: 50 mg MAG/OA/CS were dispersed in water and then, 1.5 mL of an aqueous solution of GA (25% m/v) were added. After 2 h of reaction at 45 °C under ultrasound, the sample was washed three times with water and dried at 45 °C in an oven. This formulation is named as N2 (MAG/OA/CS-G) hereafter.

An exhaustive characterization of MNPs has been performed in previous works including FTIR, XRD, magnetic measurements, and composition by ICP.[11–13]

In this work, N1 and N2 were further characterized by Dynamic Light Scattering (DLS), using a Malvern Zetasizer to determine particle hydrodynamic diameters (D_h) and surface charge by measurements of zeta potential (ζ). The measurements were performed employing aqueous dispersions of 0.1 mg MNPs/mL at 25 °C. Data are expressed as mean \pm S.D. of

ten measurements. The morphology was analyzed by transmission electron microscopy (TEM) using a JEOL100 CXII microscope (JEOL, TOKIO, Japan) from CCT, Bahía Blanca, Argentina from the same aqueous dispersions.

2.3. Animals

ECs primary cultures were obtained from young Wistar rats (1–2 months old and 150 g of weight). For the *in vivo* biodistribution experimental assays, eight weeks old CF1 female mice were used. All animals were maintained under constant conditions of temperature (22 ± 1 °C) and humidity (70%), in 12 h light: 12 h dark cycles during all the experiment. All animals had free access to tap water and standard diet throughout the experiment. The care and handling of the animals were performed in the animal facility from the Biology, Biochemistry, and Pharmacy Department of the National University of South in accordance with the internationally accepted standard Guide for the Care and Use of Laboratory Animals as adopted and promulgated by the National Institute of Health.[15] The protocols employed for this study have been approved by the CICUAE (Institutional Committee for the Care and Use of Experimental Animals, Biology, Biochemistry, and Pharmacy Department of the National University of South).

2.4. Cell culture and treatment with the MNPs

Primary cultures of ECs were obtained from aortic rings explants isolated from young Wistar rats (1–2 months old and 150 g of weight).[16] Briefly, animals were euthanized by cervical dislocation and the full length thoracic aorta was aseptically removed. Immediately after, the aorta was cleaned of adherent connective tissue, and cut into small ring-shaped segments. Ring explants were seeded in 60 mm matrix-coated Petri dishes containing phenol red-free DMEM supplemented with 20% (v/v) FCS, 60 µg/mL penicillin, 2.5 µg/mL amphotericin-B, 2 mM L-glutamine, and 1.7 g/L sodium bicarbonate. Explants were incubated at 37 °C in 5% CO₂ atmosphere. In order to establish a pure culture, after three days of culture the ring explants were removed and ECs were allowed to reach confluence. The identification of the ECs was determined by: (a) phase-contrast microscope observation of the characteristic cobblestone morphology of the confluent monolayer; (b) by positive immunoreactivity for CD34, and (c) by the bioability to synthesize NO.[17] Cells from passages 2–7 were used for all experiments. Culture medium was replaced with fresh medium containing 10% (v/v) FCS every 72 h.

2.4.1. Measurement of NO production

ECs were seeded on 24-multiwell culture plates (NUNC) at a density of 3.5×10^4 cells/well and allowed to grow to 90% of confluence in DMEM containing 10% (v/v) FCS. Nanoparticles dispersions were prepared using tapped water as solvent. Treatment was performed in fresh DMEM containing 2% (v/v) FCS, achieving final concentrations of 1, 10, and 100 µg MNPs/mL of medium for N1 and N2. Each concentration for both formulations was analyzed in triplicate. A control was also processed, where no MNPs were introduced (vehicle alone). Nitrites (NO₂⁻) were measured in the incubation media as a stable and non-volatile breakdown product of the NO released, employing the spectrometric Griess reaction.[18] Once finished treatment, aliquots of culture medium supernatant were mixed

with Griess reagent (1% sulfanilamide and 0.1% naphthylenediaminedihydrochloride in 2.5% phosphoric acid) and incubated 10 min at room temperature. Absorbance was measured at 520 nm in a BiotekSinergy-HT microplate reader. The concentration of NO_2^- in the samples was determined with reference to a sodium nitrite (NaNO_2) standard curve performed in the same matrix. Cells were dissolved in 1-M NaOH, and protein content was measured by Lowry Method.[17] The results were expressed as nmol of NO_2^- per mg of protein.

To evaluate ECs response to the NO production agonist Acetylcholine (ACh), cells were exposed to 10- μM ACh for 30 min and NO production was determined by Griess reaction.

2.4.2. Cell viability

Cell viability was measured by MTT assay (Sigma-Aldrich). Briefly, cells were seeded onto a 96-well plate (1×10^4 cells per well) and incubated for 24 h in 100 μl of DMEM with 2% FCS. Cells were treated with different concentrations of the nanoparticles or vehicle alone for 48 h. After treatment, 10 μl of MTT reagent were added to each sample and the plate was incubated in darkness in an incubator at 37 $^\circ\text{C}$ in a 5% CO_2 atmosphere for 4 h. After incubation, the medium was removed and 100 μl of dimethyl sulfoxide (DMSO) were added to each well. Absorbance was measured at 550 nm in a multiplate reader (BiotekSinergy-HT) using 690 nm as reference. Results were expressed as optical density (O.D.).

2.5. Biodistribution

2.5.1. In vivo experimental assays

The biodistribution study was performed in healthy, eight weeks old CF1 female mice. Mice were randomly divided according to the body weight (approximately 30 g) into different groups of 8 animals. Aqueous dispersions of N1 and N2 nanocarriers were administered via intraperitoneal (IP) injection. The control group received vehicle alone. The doses applied were about 30 mg MNPs/kg considering physiological doses applicable to future clinical studies. After 24 h in the acute study and after 28 days in the sub-acute assay, mice were euthanized by cervical dislocation and organs were extracted in order to evaluate the concentration of MNPs. Brain, heart, liver, kidneys, and lungs were conditioned by fixing in formalin (10%) for 24 h followed by serial dehydration in aqueous solutions of ethanol (70, 80, 96% and 100%v/v), 2 h each step.

2.5.2. MNPs quantification in organs

Quantification of MNPs in organs was performed employing the method developed by Zysler et al. [19] Magnetization versus magnetic field (-10 kOe – 10 kOe) at room temperature was measured using a commercial Vibrating Sample Magnetometer (VSM).

2.6. Statistical analysis

Comparisons between two means were performed using Student's t-test and multiple comparisons by one-way ANOVA, followed by Fisher least significant difference. p values lower than 0.05 were considered to be statistically significant.

3. Results and discussion

3.1. Characterization of the obtained formulations

MNPs are composed by almost 56% of magnetite and 44% of chitosan, oleic acid, and glutaraldehyde.[13] In previous work, we have demonstrated the necessity to better fix chitosan onto the magnetic core to avoid disaggregation. Stability studies performed by UV-Visible spectroscopy, size measurements, [12,13] and TEM analysis have demonstrated instability of chitosan coating.

Hydrodynamic diameter (Dh) and zeta potential measurements (ζ) were performed in aqueous dispersions at pH near 7.4 aiming to reproduce physiological medium. The recorded data are listed in Table 1. Results are in agreement with reported data regarding to similar formulations.[12,13] In both cases, the polydispersion indexes registered for all measurements were under 0.5, indicating that N1 and N2 rendered almost monodispersed particles in water.

The lower size of N2 in comparison to N1 is due to the stabilization imparted by glutaraldehyde cross-linking. Cross-linking reaction occurs by the formation of stable imine bonds among terminal amine groups of chitosan and aldehydic groups of glutaraldehyde. These bonds fix chitosan on the magnetite surface, imparting smaller size and more stability to the nanoparticles.[13] Anyway, the size of both systems is appropriate for their use in biomedical applications.

In Figure 1, TEM micrographs corresponding to both nanocarriers are observed. A scheme of the most probable structure of MNPs is also represented in this Figure. These data reveal that magnetic core size is around 10 nm for both formulations. Figure 2 shows the magnetic characterization results for both, N1 and N2 samples in powder form. The curves obtained are typical of superparamagnetic systems. Magnetization saturation (Ms) values were 35.5 emu/g for N1 and 40.4 emu/g for N2.

3.2. Effects on endothelial cells

In Figure 3, micrographs of ECs exposed to 1, 10, and 100 $\mu\text{g/mL}$ of N1 and N2 for 24 h are shown. As can be seen, MNPs treatment did not induce alterations in cell morphology compared to control group.

3.2.1. Effect of MNPs on endothelial NO production

The effect of different doses (1, 10, and 100 $\mu\text{g/mL}$) of N1 or N2 was examined in terms of the NO production. Figure 4(a) demonstrates that the presence of MNPs did not affect basal NO production since no statistical differences were detected between control and treated groups. It is known that acetylcholine is a physiological regulator of endothelial nitric oxide synthase (eNOS) that stimulates NO synthesis in a few minutes. As can be observed in Figure 4(a), Ach significantly enhanced NO production (54.0% above the control). In

Table 1. Hydrodynamic diameter (Dh) and zeta potential (ζ) measurements of N1 and N2 in aqueous dispersions. Results are expressed as media \pm standard deviation ($X \pm S.D.$) of 10 measurements.

Nanocarrier	Dh/ $X \pm SD$ (nm)	$\zeta/X \pm SD$ (mV)
N1	369 \pm 68	-10.5 \pm 0.9
N2	238 \pm 64	-14.8 \pm 1.1

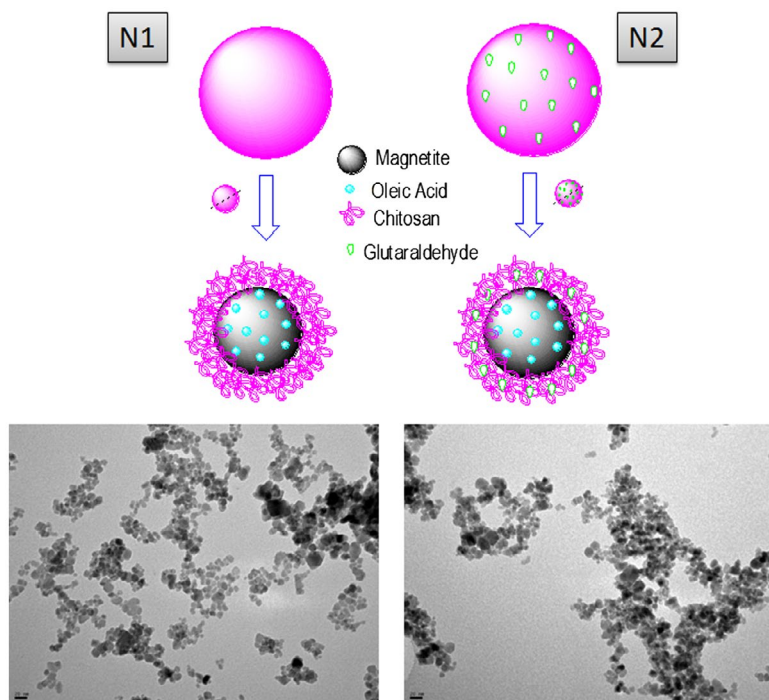


Figure 1. Schemes corresponding to the composition and morphology proposed for N1 and N2 and TEM micrographs (bar denotes a scale of 20 nm; 2700x).

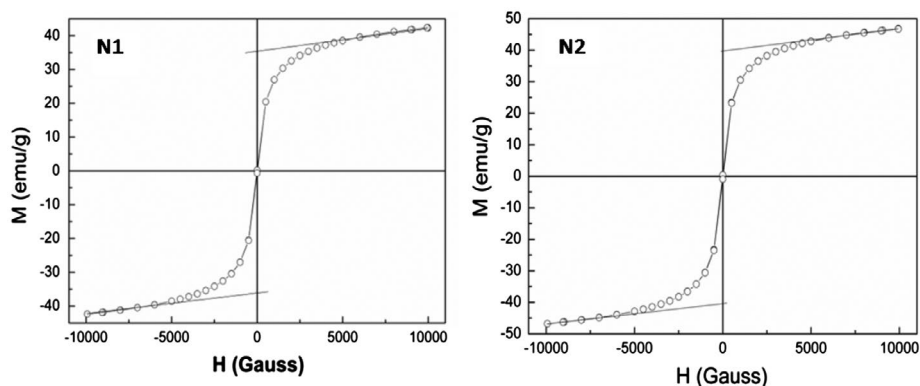


Figure 2. $M(H)$ curves corresponding to the samples N1 and N2 measured at 300 K. The line extrapolated to $H = 0$ determines the saturation magnetization (M_s) value.

the presence of N1 (24 h), the ability of ECs to respond to their natural agonist ACh was sustained. Similar results were observed when ECs were treated with different doses of N2 (Figure 4(b)).

Endothelial NO is the main regulator of vascular tone and homeostasis, and it represents one of the major markers of ECs function. Under physiological conditions, it is synthesized through the conversion of L-arginine to L-citrulline and NO by eNOS. Regulation of eNOS

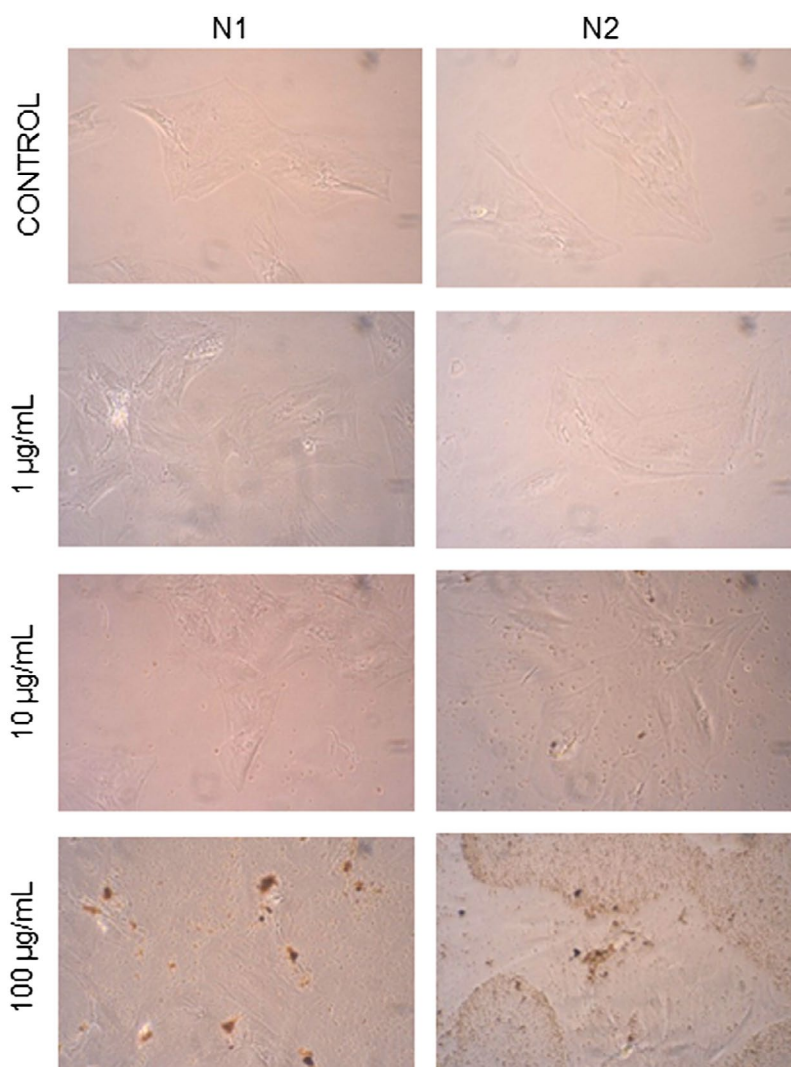


Figure 3. Endothelial cells morphology after 24 h exposure to N1 or N2. Micrographs of representative fields at 20X of each condition.

induced by physiological vascular agonists such as acetylcholine, bradikynin, and hormones is critical to maintain healthy properties of vascular wall.[4]

The presented data show that endothelial NO production is not affected by the exposure to N1 or N2. Moreover, the presence of the MNPs did not alter the ability of the cells to respond to their endogenous agonist (ACh). Indeed, no differences in cell morphology were detected neither. The combination of these results suggests that metabolism and integrity of the ECs remain intact under the treatment with the nanodevices. After a brief survey of available literature, it was found that these data are relevant since many magnetic nanosystems alter NO production on ECs.

Astanina et al. [3] evaluated the effect on ECs of Endorem[®], which is an approved formulation as an intravenous contrast agent composed of dextran-stabilized superparamagnetic

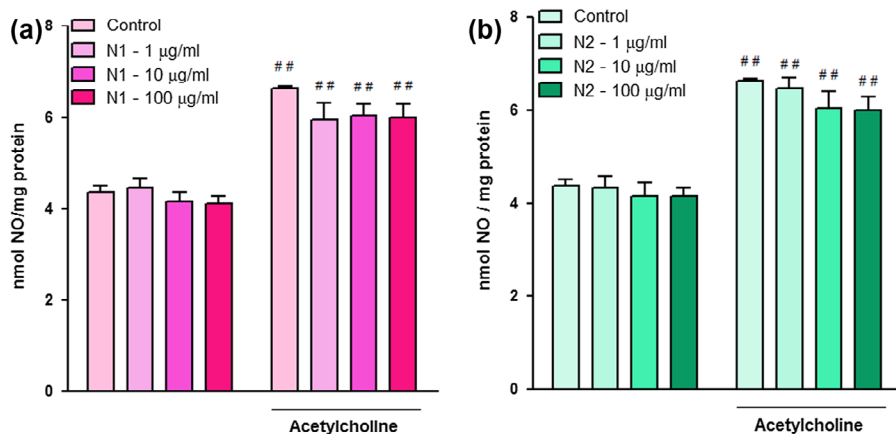


Figure 4. Effects of N1(a) and N2 (b) nanoparticles on endothelial NO production. Starved ECs were treated with nanoparticles (1, 10 or 100 µg/mL) for 24 h. Immediately after the monolayers were exposed to 10 µM ACh or vehicle alone for 30 min. Results are expressed as mean \pm SD. ## $p < 0.01$, ACh untreated vs. ACh treated cells.

nanoparticles. In this work, the MNPs were tested on human microvascular endothelial cell line, causing a diminution in NO production. The authors concluded that dextran-coated MNPs exert a cytotoxic effect on human ECs by attenuation of cytoprotective NO production.

3.2.2. Cell viability

Tetrazolium dye assay (MTT) was employed to evaluate cell viability after exposure to the nanoparticles. Only living cells can reduce the MTT to formazan, which may be quantified spectrophotometrically after dissolution in DMSO at 550 nm. The data obtained from this assay are considered indicators of cell survival.[20]

Different doses (1, 10, and 100 µg/mL) and times of exposure (6, 24 and 36 h) were assayed for each nanodevice. This assay was performed until 36 h considering that after 24 h MNPs achieve different organs (see later); so this time is sufficient enough to study the impact on ECs because the real contact time of the MNPs with ECs is lower. As shown in Figure 5, maximal cell viability was detected when ECs were treated with N1 nanoparticles for 6–24 h, compared to control cells (100%). A significant reduction in cell viability was evidenced in the treatment with the highest dose (100 µg/mL) after 36 h.

The treatment with N2 MNPs did not affect cell viability in the whole range of doses and times explored (Figure 5(b)).

In general, the cytotoxicity attributed to MNPs is considered dose-dependent [21] and it is associated to an imbalance of cytoplasmic iron ions which may cause oxidative stress leading to cellular toxicity, impaired cell metabolism, and concomitant increment in apoptosis.[2]

Iron is a natural occurring ion in the body and several mechanisms involved in its metabolism are known and described.[22] Iron from MNPs may be gradually cleared and degraded to Fe^{3+} by different endogenous metabolic pathways. Then it would enter the pool of body iron to be used in the generation of red blood cells. The excess is excreted by the kidneys.[23]

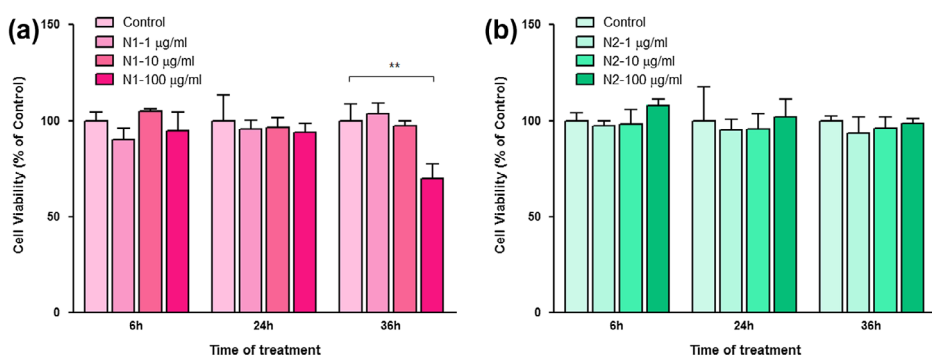


Figure 5. Viability of ECs incubated with N1 (a) and N2 (b) nanoparticles from three independent experiments. Cells were exposed to the indicated concentrations of nanoparticles for 6, 24, or 36 h. Data are expressed as mean \pm SD. ** $p < 0.01$ vs. Control.

The different effect on cell viability observed for N1 and N2 at highest doses and after 36 h of treatment can be attributed to the composition of the formulations, especially to the structure of chitosan coating. So therefore, the reduction in cell survival exerted by N1 at the dose of 100 $\mu\text{g}/\text{mL}$ could be due to the possible disaggregation of chitosan in the cytoplasm of the ECs, exposing high quantities of iron ions from the magnetic core of the MNPs. In previous research, we have demonstrated that non-cross-linked chitosan is feasible to disaggregate from the surface of the nanomagnetite. GA cross-linking leads to the formation of stable imine bonds between chitosan moieties, improving the stability of the coating.[13]

Berry et al. [24] observed that dextran-coated magnetite nanoparticles-induced cell death and diminished proliferation when primary human fibroblasts were exposed in culture to doses of 50 $\mu\text{g}/\text{mL}$. Even though they expected that coated magnetite would not cause cellular damage (as dextran is not noted for cytotoxic effects directly), they observed similar results in comparison to naked magnetite nanoparticles. These effects were justified considering that dextran shell on the particles could be broken down, exposing iron or particles aggregates which may influence cellular processes.[25]

Naqvi et al. [26] demonstrated by MTT assays that SPIONs coated with Tween 80 exerted cytotoxicity in murine macrophage (J774) cells. SPIONs reduced to near 60% the cell viability at doses up to 200 $\mu\text{g}/\text{mL}$ after only six hours of treatment. In the cases of N1 and N2, it is evident that chitosan coating raised cytocompatibility since the reduction in cell viability was observed after 36 h of exposure. N2 would result a better nanocarrier compared with N1. This behavior may be ascribed to the stabilization imparted by cross-linking of the biopolymer with glutaraldehyde.[13] Cross-linking would fix chitosan chains on the magnetic core avoiding iron direct exposition. Then, this strategy in the coating of the magnetic core would prevent from iron-induced cellular oxidative stress, not affecting cell viability. In general, it is considered that MNPs are transported by transcitosis in ECs.[27] So it is expected that they could cross the cytoplasm without exerting cytotoxicity. It may be postulated that the combination of high concentration, long-time exposure, and unstable coating would be the responsible of viability reduction using 100 μg MNPs/ mL dose during 36 h. Potential saturation of transport mechanisms would lead to cytoplasmic accumulation of the MNPs with concomitant development of iron toxicity.

It is important to highlight that according to the achieved results, glutaraldehyde does not exert cytotoxicity on ECs at the doses contained in the concentration of MNPs studied. In general, glutaraldehyde can act as a cytotoxic substance by inducing apoptosis. Such is the case of the research developed by Gough et al. [28] where the cross-linking with glutaraldehyde on collagen/poly(vinyl alcohol) bioartificial composite films induced apoptosis on human osteoblasts. Our finding is consistent with previous studies reported by Ma et al. [29] They obtained a chitosan/collagen scaffold by cross-linking with glutaraldehyde and proposed that the potential cytotoxicity of glutaraldehyde might be decreased by the presence of chitosan, obtaining a biocompatible material, nontoxic for fibroblasts.

3.3. Tissue distribution

Figure 6 shows characteristic curves corresponding to the superposition of a superparamagnetic system signal. It is observable the absence of MNPs in control brain, where saturation magnetization is equivalent to zero. Liver corresponding to a mouse treated with N1 reveals the presence of MNPs, meanwhile saturation magnetization is low in a brain of a mouse treated with N2. This indicates low concentration of N2 in this sample. The saturation magnetization of the MNPs, and consequently their mass in each organ, were determined by the analysis of the curves extrapolating the high magnetic fields data to zero fields. This method developed by Zysler et al. [19] presents the advantage of high accuracy to determine the content of MNPs without the contribution of endogenous iron in the tissue or blood.

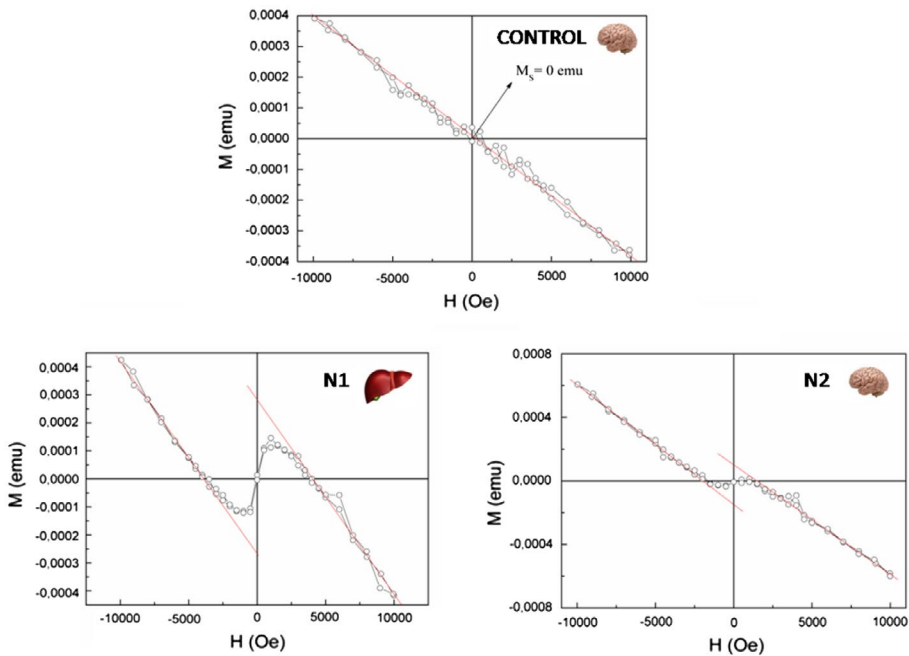


Figure 6. Representative magnetization curves obtained from the VSM measurements on brain and liver of mice, after 24 h of IP administration with MNPs. Doses of N1 and N2 were equivalent to 30 mg MNPs/kg. Control corresponds to animal that received no treatment with nanocarriers.

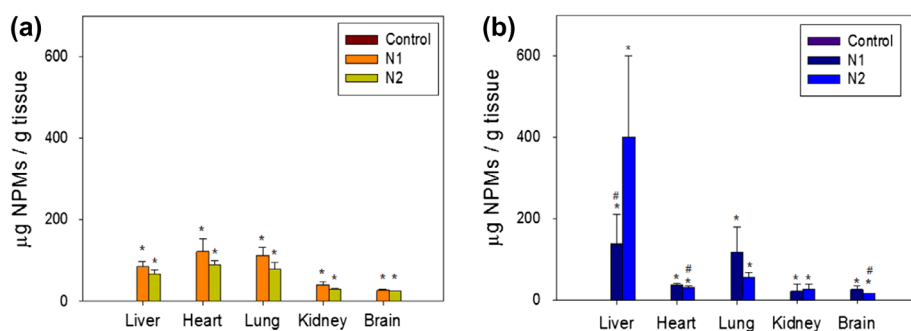


Figure 7. (a) Biodistribution of N1 and N2 after 24 h of IP injection in mice; (b) Biodistribution of N1 and N2 after 28 days of a weekly IP administration in mice.

Note: * $p < 0.05$ with respect to the control group. # $p < 0.05$ with respect to the same organ studied after the acute biodistribution. Results are expressed as \bar{X} (media) \pm S.E.M. (standard error of media).

Quantification of N1 and N2 in the explored organs is shown in Figure 7, establishing the acute (a) and the sub acute (b) biodistribution patterns of the nanosystems.

The aim of the acute biodistribution assay is to evaluate the acute body distribution in order to gain knowledge about the organs where these MNPs are preferably distributed by bloodstream in a short period of time. These data are relevant to future studies related to biomedical magnetic targeting, considering the targeting an acute practice after MNPs administration.

N1 and N2 were distributed to diverse organs after 24 h from IP administration. The highest quantity of both nanocarriers was found in heart. Then, lungs and liver were the tissues where the MNPs were preferentially distributed, while kidneys and brain contained the lowest quantity.

Regarding to the biodistribution after 28 days of treatment, no significant differences were observed among N1 and N2 in the organs reached by each formulation. However, significant differences were found concerning the amount of nanoparticles deposited in some organs with respect to acute assay.

After IP administration, it is expected that the major quantity of MNPs would be taken up by the liver due to the first-pass effects, and would be later redistributed to other organs. [30] It is also expected that *in vivo* injected MNPs would be captured by macrophages from the RES, reducing blood circulation time and rendering accumulation in liver (80–90%). [31] Unexpectedly, low percentages of both N1 and N2 MNPs were found in liver (15 and 14.5%, respectively). These data suggest that these MNPs would be redistributed from liver, avoiding significantly the capture by the RES after 24 h from IP administration. This behavior would improve the blood circulation time of the carriers.

In general, various characteristics associated to the morphology of NPs are implicated in the biodistribution profile besides RES. Regarding to the size, it is expected that larger NPs would be quickly taken up by the liver, imparting short circulation time in blood. On the contrary, smaller MNPs present easier access to other organs and longer circulation time.[32,33]

Biodistribution of superparamagnetic iron oxide nanoparticles (SPIONs) has been studied regarding to the *in vivo* effect of size. For instance, Chouly et al. [34] studied dextran-coated SPIONs ranging in size from 33 to 90 nm. They have found that larger ones

exhibit faster and greater uptake in the liver. Jain et al. [6] analyzed the biodistribution of Pluronic-OA-SPIONs with particle sizes around 193 nm. They observed that the 55% of the initial dose was distributed to the liver, demonstrating that the Pluronic-OA-SPIONs were taken up by the RES. Mojica Piscioti et al. [8] have studied dextran- and polyethylene glycol-coated SPIONs and their biodistribution profile in mice. The hydrodynamic diameters of these particles were estimated in 170 and 120 nm for the Dextran- and PEG-coated systems. The study revealed that largest amounts of MNPs were found in liver.

The nanosystems studied in this work present Dh of 369 nm (N1) and 238 nm (N2), indicating that even when they are larger than other reported NPs, they are able to avoid the capture by RES of liver. By this way, other factors than size would be responsible for tissue distribution. This result reinforces the hypothesis that not only RES is responsible for the capture, but also the chemical structures of MNPs. Fundamentally, particles coating would play a crucial role in biodistribution.[7] In this regards, chitosan would influence the interactions among the nanoparticles and RES. The supramolecular structure of the biopolymeric coating is plausible to generate hindrance to macrophage ability to phagocytose MNPs. The surface charge is another important parameter which influences the biodistribution of MNPs. Neutral NPs result the most adequate because they tend to avoid RES capture due to a decrease in opsonisation [35]. Papisov et al. [36] studied positively charged (poly-lysine)-dextran-coated SPIONs which showed a rapid clearance by liver; meanwhile negatively charged succinate-(poly-lysine) dextran-coated SPIONs presented an incremented blood circulating time and exhibited a biodistribution profile similar to nearly neutrally charged dextran-coated SPIONs. In this case, both N1 and N2 present a negative surface charge at physiological conditions (Table 1). This characteristic would possibly contribute to the low capture by the RES in the liver.

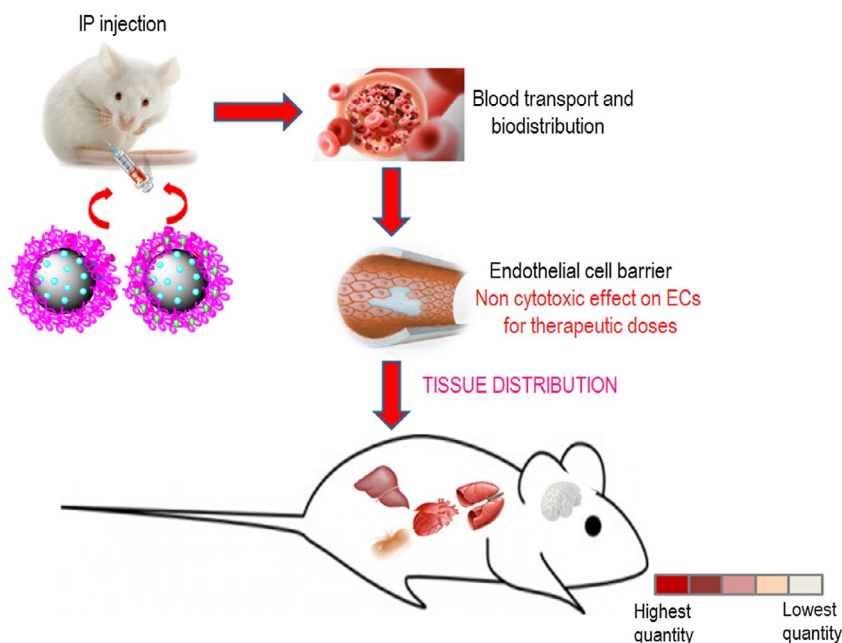
On the other hand, not only the intrinsic features of the MNPs determine biodistribution, but also physiology and histology of the organs. By this way, it is also important to evaluate biodistribution in terms of the tissue characteristics. It is observable that N1 and N2 reached greater quantity in lung and heart compared to those observed in the rest of the organs studied. This could be ascribable to the high blood irrigation of these organs. The endothelium of muscle and lung capillaries presents a continuous morphology that permit small molecules to be transported across the capillary wall.[37]

The clearance of NPs by the kidneys depends on several factors such as size and surface charge. Particles with hydrodynamic diameters smaller than 8 nm may be filtered by the glomerular capillary membrane and then would be cleared by the urine.[38] Negatively charged particles may fail to pass through the pores of the membrane because of the negatively charged pores.[22] N1 and N2 were found in small quantities in kidney, in agreement with these features.

The low concentrations of N1 and N2 quantified in brain suggest that they are not able to cross the blood-brain barrier in high quantities, at least in short periods of time after administration.

The analysis of the acute biodistribution patterns of N1 and N2 revealed that there are not significant differences between both nanocarriers. Glutaraldehyde cross-linking in N2 would not have impact on the tissue specificity after 24 h from injection. In Scheme 8, it is shown the acute biodistribution profile for the magnetic nanocarriers in the organs studied.

After weekly administration during 28 days, concentration of both N1 and N2 was incremented in liver. This situation is attributable to the repetition of the initial dose after



Scheme 1. MNPs studied were administered via IP injection. After reaching blood stream and crossing the endothelial barrier, they are biodistributed to the whole organism. The magnetic devices do not affect ECs at therapeutic doses. The formulations greatly avoided the initial clearance by liver reticulo-endothelial system (RES), in comparison to several other nanoparticulated carriers after 24 h from IP administration.

the studied time. This increase indicates that after repeated doses over time, liver would act as detoxification system of these formulations. Moreover, repeated doses could cause liver bioaccumulation. This fact is important to consider when applying these MNPs for chronic treatments. It is worth mentioning that N2 has been found in greater concentration than N1 in liver. One hypothesis is based on the stabilization imparted by chitosan cross-linking. This phenomenon would delay the elimination of the nanoparticles in the liver by protecting from exposure of the magnetic core. Just as the cross-linking protects endothelial cells from oxidative stress caused by possible iron overload, it is possible that the mechanisms of liver detoxification do not recognize N2 as toxic systems, thereby retarding their elimination.

The concentration of both N1 and N2 decreased significantly in the heart after subacute administration in comparison to the concentrations found after the acute exposure. These results reveal that after a more sustained exposure over time, the chitosan-coated MNPs decrease circulation in bloodstream and remain deposited in various organs. This finding confirms that the highest concentration found in heart after the acute study would be due to high blood supply to heart. And also, to the increased circulation time given by the chitosan coating which avoids from acute clearance by RES.

A significant decrease in the concentration of N1 and N2 in the heart was also observed after the subacute exposure. A similar behavior was evidenced for N2 in brain. These findings constitute a significant contribution in terms of the knowledge about the possible metabolism of these MNPs, revealing that chitosan-coated MNPs would not accumulate in these organs after repeated applications. These organs would be able to metabolize or

eliminate them efficiently. In this last case, the liver might be responsible for disposal according to the observed increase in the concentration.

5. Conclusion

The information recovered from this research demonstrated that MNPs composed of magnetite/chitosan and magnetite/chitosan/glutaraldehyde do not affect ECs metabolism. The nanocarrier N2 does not induce cytotoxicity on ECs, meanwhile N1 diminishes cell viability at the highest explored dose and longer treatment times. The differences found are attributable to the chemical composition of the carriers, revealing a close relationship among physicochemical properties and biological behavior. Cross-linked chitosan with glutaraldehyde prevents from chitosan disaggregation, avoiding the direct exposure to iron from the magnetic core. This strategy on coating would prevent from iron associated cytotoxicity.

The acute biodistribution profile in different mice organs resulted similar for N1 and N2. It is noticeable that both nanocarriers greatly avoided the initial clearance by RES in liver, in comparison to other reported MNPs. This characteristic is attributable to the surface charge and the controlled size as imparted by the coating of the magnetic core. The sub acute exposure to N1 and N2 revealed an increment in the concentration of both nanosystems in liver and a concomitant decrease in heart and brain (in special N2). This indicates that after repeated doses the MNPs did not accumulate in the organs. Besides, liver could be the possible site of detoxification.

MNPs as drug-targeted devices represent a promising advance in the located treatment of several diseases. The improvement in the knowledge about the behavior of these nanosystems *in vitro* and *in vivo* is essential for the understanding of their metabolism and toxicity; both important features for the employment of these novel biomaterials. Morphological, magnetic, and biological properties found for N1 and N2 reveal them as likely nanodevices for the magnetic guidance of drugs to specific desired sites of the organism.

Disclosure statement

No potential conflict of interest was reported by the authors.

Funding

This work was financially supported by the CONICET (Argentina) and the PGI N° 24/ZQ09 (UNS, Argentina).

References

- [1] Mahmoudi M, Hofmann H, Rothen-Rutishauser B, et al. Assessing the *in vitro* and *in vivo* toxicity of superparamagnetic iron oxide nanoparticles. *Chem. Revs.* 2011;112:2323–2338. doi:<http://dx.doi.org/10.1021/cr2002596>.
- [2] Markides H, Rotherham M, El Haj AJ. Biocompatibility and toxicity of magnetic nanoparticles in regenerative medicine. *J. Nanomat.* 2012;2012:13. doi: <http://dx.doi.org/10.1155/2012/614094>.
- [3] Astanina K, Simon Y, Cavelius C, et al. Superparamagnetic iron oxide nanoparticles impair endothelial integrity and inhibit nitric oxide production. *Acta Biomater.* 2014;10:4896–4911. doi:<http://dx.doi.org/10.1016/j.actbio.2014.07.027>.

- [4] Michiels C. Endothelial cell functions. *J. Cell. Physiol.* **2003**;196:430–443. doi:<http://dx.doi.org/10.1002/jcp.10333>.
- [5] Ge G, Wu H, Xiong F, et al. The cytotoxicity evaluation of magnetic iron oxide nanoparticles on human aortic endothelial cells. *Nanoscale Res. Lett.* **2013**;8:215. doi:<http://dx.doi.org/10.1186/1556-276X-8-215>.
- [6] Jain TK, Reddy MK, Morales MA, et al. Biodistribution, clearance, and biocompatibility of iron oxide magnetic nanoparticles in rats. *Mol. Pharm.* **2008**;5:316–327. doi:<http://dx.doi.org/10.1021/mp7001285>.
- [7] Cole AJ, David AE, Wang J, et al. Magnetic brain tumor targeting and biodistribution of long-circulating PEG-modified, cross-linked starch-coated iron oxide nanoparticles. *Biomaterials.* **2011**;32:6291–6301. doi:<http://dx.doi.org/10.1016/j.biomaterials.2011.05.024>.
- [8] Mojica Piscioti ML, Lima E Jr, Vasquez Mansilla MM, et al. In vitro and *in vivo* experiments with iron oxide nanoparticles functionalized with DEXTRAN or polyethylene glycol for medical applications: magnetic targeting. *J. Biomed. Mater. Res. B Appl. Biomater.* **2014**;102:860–868. doi:<http://dx.doi.org/10.1002/jbm.b.33068>.
- [9] Almeida JPM, Chen AL, Foster A, et al. *In vivo* biodistribution of nanoparticles. *Nanomedicine.* **2011**;6:815–835. doi:<http://dx.doi.org/10.2217/nnm.11.79>.
- [10] Donaldson K, Stone V, Tran CL, et al. *Occup. Environ. Med.* **2004**;61:727–728. doi:<http://dx.doi.org/10.1136/oem.2004.013243>.
- [11] Nicolás P, Saleta M, Troiani H, et al. Preparation of iron oxide nanoparticles stabilized with biomolecules: experimental and mechanistic issues. *Acta Biomater.* **2013**;9:4754–4762. doi:<http://dx.doi.org/10.1016/j.actbio.2012.09.040>.
- [12] Agotegaray M, Palma S, Lassalle V. Novel chitosan coated magnetic nanocarriers for the targeted diclofenac delivery. *J. Nanosci. Nanotechnol.* **2014**;14:3343–3347. doi:<http://dx.doi.org/10.1166/jnn.2014.8256>.
- [13] Agotegaray M, Lassalle V. Study of the experimental conditions and mechanisms for diclofenac loading in functionalized magnetic nanoparticles. *Int. J. Chem. Pharm. Anal.* **2014**;1: 154–164. <http://www.pmindexing.com/journals/index.php/IJCPA/article/view/288>.
- [14] Kim DH, Lee SH, Im KH, et al. Biodistribution of chitosan-based magnetite suspensions for targeted hyperthermia in ICR mice. *IEEE Trans. Magn.* **2005**;41:4158–4160. doi:<http://dx.doi.org/10.1109/INTMAG.2005.1463997>.
- [15] National Research Council. *Guide for the care and use of laboratory animals*. Washington (DC): National Academies Press; **2011**.
- [16] Yeh YC, Hwang GY, Liu IP, et al. Identification and expression of scavenger receptor SR-BI in endothelial cells and smooth muscle cells of rat aorta in vitro and *in vivo*. *Atherosclerosis.* **2002**;161:95–103. doi:[http://dx.doi.org/10.1016/S0021-9150\(01\)00642-6](http://dx.doi.org/10.1016/S0021-9150(01)00642-6).
- [17] Campelo AE, Cutini PH, Massheimer VL. Cellular actions of testosterone in vascular cells: mechanism independent of aromatization to estradiol. *Steroids.* **2012**;77:1033–1040. doi:<http://dx.doi.org/10.1016/j.steroids.2012.05.008>.
- [18] Lowry OH, Rosebrough NJ, Farr AL, et al. Protein measurement with the Folin phenol reagent. *J. Biol. Chem.* **1951**;193:265–275. <http://www.jbc.org/content/193/1/265.long>.
- [19] Zysler RD, Lima E Jr, Mansilla MV, et al. A new quantitative method to determine the uptake of SPIONs in animal tissue and its application to determine the quantity of nanoparticles in the liver and lung of Balb-c mice exposed to the SPIONs. *J. Biomed. Nanotechnol.* **2013**;9:142–145. doi:<http://dx.doi.org/10.1166/jbn.2013.1467>.
- [20] Mosmann T. Rapid colorimetric assay for cellular growth and survival: application to proliferation and cytotoxicity assays. *J. Immunol. Methods.* **1983**;65:55–63. doi:[http://dx.doi.org/10.1016/0022-1759\(83\)90303-4](http://dx.doi.org/10.1016/0022-1759(83)90303-4).
- [21] Boyer C, Whittaker MR, Bulmus V, et al. The design and utility of polymer-stabilized iron-oxide nanoparticles for nanomedicine applications. *NPG Asia Mater.* **2010**;2:23–30. doi:<http://dx.doi.org/10.1038/asiamat.2010.6>.
- [22] Hall JE. *Guyton and hall textbook of medical physiology*. London: Elsevier; **2010**.

- [23] Anzai Y, Piccoli CW, Outwater EK, et al. Evaluation of neck and body metastases to nodes with ferumoxtran 10-enhanced MR imaging: phase III safety and efficacy study. *Radiology*. 2003;228:777–788. doi:<http://dx.doi.org/10.1148/radiol.2283020872>.
- [24] Berry C, Wells S, Charles S, et al. Dextran and albumin derivatised iron oxide nanoparticles: influence on fibroblasts *in vitro*. *Biomaterials*. 2003;24:4551–4557. doi:[http://dx.doi.org/10.1016/S0142-9612\(03\)00237-0](http://dx.doi.org/10.1016/S0142-9612(03)00237-0).
- [25] Jordan A, Wust P, Scholz R, et al. Cellular uptake of magnetic fluid particles and their effects on human carcinoma cells exposed to AC magnetic fields *in vitro*. *Int. J. Hyperth*. 1996;12:705–722. doi:<http://dx.doi.org/10.3109/02656739609027678>.
- [26] Naqvi S, Naqvi M, Samim M, et al. Concentration-dependent toxicity of iron oxide nanoparticles mediated by increased oxidative stress. *Int. J. Nanomed*. 2010;5:983–989. doi:<http://dx.doi.org/10.2147/IJN.S13244>.
- [27] Kou L, Sun J, Zhai Y, et al. The endocytosis and intracellular fate of nanomedicines: implication for rational design. *Asian J. Pharm. Sci*. 2013;8:1–10. doi:<http://dx.doi.org/10.1016/j.ajps.2013.07.001>.
- [28] Gough JE, Scotchford CA, Downes S. Cytotoxicity of glutaraldehyde crosslinked collagen/poly(vinyl alcohol) films is by the mechanism of apoptosis. *J. Biomed. Mater. Res*. 2002;61:121–130. doi:<http://dx.doi.org/10.1002/jbm.10145>.
- [29] Ma L, Gao C, Mao Z, et al. Collagen/chitosan porous scaffolds with improved biostability for skin tissue engineering. *Biomaterials*. 2003;24:4833–4841. doi:[http://dx.doi.org/10.1016/S0142-9612\(03\)00374-0](http://dx.doi.org/10.1016/S0142-9612(03)00374-0).
- [30] Kim IY, Seo SJ, Moon HS, et al. Chitosan and its derivatives for tissue engineering applications. *Biotechnol. Adv*. 2008;26:1–21. doi: <http://dx.doi.org/10.1016/j.biotechadv.2007.07.009>.
- [31] Varna M, Ratajczak P, Ferreira I, et al. *In vivo* distribution of inorganic nanoparticles in preclinical models. *J. Biomat Nanobiotech*. 2012;03:269. doi:<http://dx.doi.org/10.4236/jbnb.2012.322033>.
- [32] Li M, Al-Jamal KT, Kostarelos K, et al. Physiologically based pharmacokinetic modeling of nanoparticles. *ACS Nano*. 2010;4:6303–6317. doi:<http://dx.doi.org/10.1021/nn1018818>.
- [33] Owens E, Peppas NA. Opsonization, biodistribution, and pharmacokinetics of polymeric nanoparticles. *Int. J. Pharm*. 2006;307:93–102. doi:<http://dx.doi.org/10.1016/j.ijpharm.2005.10.010>.
- [34] Chouly C, Pouliquen D, Lucet I, et al. Development of superparamagnetic nanoparticles for MRI: effect of particle size, charge and surface nature on biodistribution. *J. Microencapsul*. 1996;13:245–255. doi:<http://dx.doi.org/10.3109/02652049609026013>.
- [35] Aggarwal P, Hall JB, McLeland CB, et al. Nanoparticle interaction with plasma proteins as it relates to particle biodistribution, biocompatibility and therapeutic efficacy. *Adv. Drug Deliv. Rev*. 2009;61:428–437. doi:<http://dx.doi.org/10.1016/j.addr.2009.03.009>.
- [36] Papisov MI, Bogdanov A Jr, Schaffer B, et al. Colloidal magnetic resonance contrast agents: effect of particle surface on biodistribution. *J. Magn. Magn. Mater*. 1993;122:383–386. doi:[http://dx.doi.org/10.1016/0304-8853\(93\)91115-N](http://dx.doi.org/10.1016/0304-8853(93)91115-N).
- [37] Chrastina A, Massey KA, Schnitzer JE. Overcoming *in vivo* barriers to targeted nanodelivery. *Interdiscip. Rev. Nanomed. Nanobiotechnol*. 2011;3:421–437. doi:<http://dx.doi.org/10.1002/wnan.143>.
- [38] Longmire M, Choyke PL, Kobayashi H. Clearance properties of nano-sized particles and molecules as imaging agents: considerations and caveats. *Nanomedicine*. 2008;3:703–717. doi:<http://dx.doi.org/10.2217/17435889.3.5.703>.